Spectrum of metastatic and non-metastatic skeletal findings with dual-phase ^{18}F-Fluoroethylcholine PET/CT in patients with biochemical relapse of prostate cancer

Athar Haroon[1], Rizwan Syed[2], Raymond Endozo[2], Rayjanah Allie[2], Alex Freeman[3], Mark Emberton[4], Jamshed Bomanji[2]

[1]Department of Nuclear Medicine, Barts Health NHS Trust, St Bartholomew's Hospital, London, UK

[2]Institute of Nuclear Medicine, University College London Hospital NHS Trust, London, UK

[3]Department of Histopathology, University College London Hospitals NHS Trust, London, UK

[4]Division of Surgery and Interventional Science, University College London, London, UK

Dr Athar Haroon FRCR

Consultant Radionuclide Radiologist

Barts Health NHS Trust

St Bartholomew's Hospital

West Smithfield, London

EC1A 7BE

London, UK

atharharoon@yahoo.com

No institutional review board approval was obtained for this study. The patients were evaluated as imaging was performed as part of their standard of care. The abstract was presented at the British Nuclear Medicine Society Meeting in 2012.

Spectrum of metastatic and non-metastatic skeletal findings with dual-phase ^{18}F-fluoroethylcholine PET/CT in patients with biochemical relapse of prostate cancer

ABSTRACT

The aim of this study was to evaluate the spectrum of skeletal findings on dual-phase ^{18}F-fluoroethylcholine (FECH) PET/CT performed during the work-up of patients referred for suspected prostate cancer relapse.

Methods: Three hundred ^{18}F-FECH PET/CT scans were prospectively evaluated. The low-dose CT features of all cases were categorized as isodense, sclerotic, lytic, or mixed lytic/sclerotic and SUV_{max} values were calculated. Findings on ^{18}F-FECH PET/CT were correlated with ^{99m}Tc-MDP planar bone scans and serum PSA.

Results: Patient age range was 50–90 years (median 71) and PSA values, 0.04–372 ng/mL (Roche Modular method). Seventy-two lesions were detected on ^{18}F-FECH PET/CT in 45 patients, including 31 (43%) in the pelvis, 17 (23%) in the spine {cervical 3, thoracic 8 and lumbar spine 6}, and 10 (13%) in ribs. Evaluation of low-dose CT in combination with PET helped to characterize benign findings in 21 (29%) lesions. The SUV_{max} for all except one benign lesion ranged from 0.49 to 2.15. In 51 lesions (71%) due to metastatic disease, SUV_{max} was 0.6–11.6 for those classified as sclerotic on low-dose CT, 0.7–8.58 for lytic lesions, 1.1–7.65 for isodense lesions, and 1.27–3.53 for mixed lytic/sclerotic lesions. Of the 56 ^{18}F-FECH avid lesions, 21 lesions showed avidity on bone scan {3 (23%) of the 13 isodense lesions, 14 (40%) of the 35

sclerotic lesions, 2 (50%) of the lytic lesions, and 2 (50%) of the mixed sclerotic/lytic lesions}. .

Conclusion: ^{18}F-FECH PET/CT identified bone lesions in 15% of patients with suspected prostate cancer relapse. SUV_{max} in isolation cannot be used to characterize these lesions as benign or malignant. Minimal overlap of benign and malignant lesions was seen above SUVmax of 2.5. Low-dose CT of PET/CT is a useful tool to assist characterization.

INTRODUCTION

Biochemical recurrence after radical prostatectomy or radiation therapy has been reported in 27%–53% of patients [1] . Radiology and nuclear medicine techniques play an important role in the detection of local relapse and lymph node and skeletal metastases. Most institutes rely on magnetic resonance imaging (MRI) for this purpose, with increasing emphasis on the multiparametric technique. The main advantage of MRI is its excellent anatomic resolution. Nevertheless, positron emission tomography/computed tomography (PET/CT) offers benefits due to its increasing ability to demonstrate functional characteristics thereby facilitating differentiation between benign and malignant lesions. PET imaging is based on labeling of small, biologically and clinically significant molecules with positron-emitters. A variety of compounds have been used for this purpose, e.g., sugar, amino acids, nucleic acids, receptor binding ligands, water, and oxygen. Physiological maps of functions or processes relevant to the labeled molecules can be created in real time by imaging the temporal distribution of these compounds [2].

In the past decade, tremendous work has been done in elucidating the potential role of PET biomarkers in supplementing MRI for the detection of metastatic disease, including in morphologically normal lymph nodes, the bone marrow, and the skeleton. While ^{18}F-fluorodeoxyglucose (FDG) is the most common PET/CT tracer worldwide, the results in respect of prostate cancer detection are not very good [3]. Consequently, other tracers have been investigated for this purpose, and choline has emerged as one of the most common non-FDG PET biomarkers for the evaluation of prostate cancer [4] .

In a meta-analysis [5], it was found that MRI and choline PET/CT were more accurate than bone single-photon emission computed tomography (SPECT) and bone scintigraphy (BS) for detecting bone metastases in patients with prostate cancer. The sensitivity and specificity of MRI on a per-patient basis were 95% and 96%, respectively, while those of choline PET/CT were approximately 87% and 97%, respectively. Though choline PET/CT had the highest specificity on a per-patient basis, MRI was significantly better than choline PET/CT (p<0.05) and BS (p<0.05) for the detection of bone metastases from prostate cancer. The area under the curve (AUC) estimate for MRI (0.9870) on a per-patient basis was also significantly higher than those for choline PET/CT (0.9541, p<0.05) and BS (0.8876, p<0.05). On a per-lesion basis, choline PET/CT had a higher AUC (0.9494) than bone SPECT (0.9381) and BS (0.7736) .

In vitro data have demonstrated greater ^{18}F-fluorocholine than FDG uptake in androgen-dependent (LNCaP) and androgen-independent (PC-3) prostate cancer cells [6]. A meta-analysis by Shen G etal demonstrated that on a per patient basis MRI was better than choline PET/CT and bone scan. Choline PET/CT was found to have highest diagnostic odds ratio compared to bone SPECT and bone scan.

There are three commonly used choline-based tracers, namely ^{18}F-fluoroethylcholine (^{18}F-FECH), ^{18}F-methylcholine, and ^{11}C-choline, which have a similar physiological biodistribution [7] . The purpose of the current study was to evaluate the spectrum of skeletal findings on ^{18}F-FECH PET/CT in patients undergoing investigation for biochemical relapse of prostate cancer.

MATERIALS AND METHODS

A total of 300 ^{18}F-FECH PET/CT scans were prospectively evaluated for detection of skeletal findings in patients with suspected prostate cancer relapse. ^{18}F-FECH was provided by Erigal (Erigal Limited, Downs Road, Sutton, Surrey, UK), synthesized as described by Hara et al. [8] . All QC parameters were fulfilled during the commercial preparation. Patients were injected with 300–370 MBq of ^{18}F-FECH (effective dose 12.95 mSv). Whole-body PET/CT images were acquired 60 min after tracer injection. A 90-min post-injection dedicated view of the pelvis was also obtained. Owing to the rapid excretion of ^{18}F-FECH in urine, patients were asked to empty their bladder prior to imaging. The CT acquisition parameters included: scout 120 kVp, 10 mA; CT 140 kVp, 80 mA, 0.8 s, pitch 1.75; CT slices 5 mm (70-cm FOV PET AC), 2.5 mm (50-cm FOV Std), 2.5 mm (50-cm FOV Lung). PET acquisition parameters were: 3D attenuation-

corrected and non-attenuation-corrected images, 20 subsets with iterative reconstructions. CT images were used to produce attenuation correction values for PET emission reconstruction and fused PET/CT presentation. The images were read by a nuclear medicine physician (with 20 years' experience) and a radionuclide radiologist (with 5 years' experience). The low-dose CT features of all cases were categorized into four groups (isodense, sclerotic, lytic, and mixed lytic/sclerotic) and maximum standardized uptake values (SUV_{max}) were calculated. Planar bone scan images were acquired after intravenous injection of ^{99m}Tc-methylene diphosphonate (MDP) and correlation was made with ^{18}F-FECH PET/CT for detection of skeletal lesions.

Benign lesions on PET/CT were those which were situated at sites of previous trauma, joints with arthritic changes (loss of disc space, peri-articular sclerosis, sub-articular cyst formation, peri-articular osteophytes), intervertebral discs with degenerative changes, facial sinuses with features of sinusitis, avascular necrosis, thickened cortex with bone expansion and coarse trabecular pattern (Paget's disease) and ground glass change (fibrous dysplasia). Malignant lesions had 18F FECH avidity, intramedullary location and associated altered morphology i-e sclerotic, lytic or mixed pattern. The identification of these lesions was based on subjective assessment.

If the lesion is not metabolically active but showed CT abnormality this either reflects a non viable lesion or apoptosis. Lesions which are found to be *suspicious* on PET/CT and there is concordance with other imaging modalities are considered *highly suspicious* for metastatic disease For the purpose of this study (in the absence of histology) we have relied on the avidity of the lesions on PET

component as gold standard. At the same time we have highlighted the weakness of the gold standard. This reflects challenges faced by the radiologists and nuclear medicine physicians in multidisciplinary team settings.

RESULTS

The age range of the 300 patients was 50–90 years (mean 71.3 years) and PSA values were 0.04–372 ng/mL (Roche Modular method). A total of 72 lesions were detected on ^{18}F-FECH PET/CT in 45 patients (15%).

Anatomically the distribution of lesions was similar to what is seen in cases of metastatic prostate cancer. In our study of the 72 lesions, 31 were found in the pelvis, 17 in the spine (cervical 3, thoracic 8 and lumbar spine 6), 10 in ribs, 4 in the sternum, 3 in bone marrow, 3 in the skull, 2 in the scapula, 1 in the clavicle, and 1 in the femur.

The final interpretation of the lesions as benign or malignant on ^{18}F FECH PET/CT was based on overall anatomical appearances of the lesions and avidity (Fig 1a). Benign findings (21/72) included bone island (13), avascular necrosis (1), fibrous dysplasia (1), Paget's disease (1), vertebral fractures (2), advanced focal degenerative changes (2), and inflammatory changes (maxillary sinus) (1). The SUV_{max} for vast majority of benign lesions ranged from 0.49 to 2.15. Only one case in this case cohort, with fibrous dysplasia, had very high SUV_{max} (10.8).

The malignant lesions were further subcategorized based on anatomical appearances on the low dose CT as isodense, sclerotic, lytic and mixed lytic or sclerotic lesions. A total of 51 lesions were considered to be of malignant etiology. The SUV_{max} values for the malignant lesions ranged from 0.6 to 11.6. The lytic lesions had SUVmax in the range of

2.36-8.58, sclerotic lesions 0.6-11.6, isodense lesions 2-7.65 and mixed lytic/sclerotic lesions as 2.75-3.53. There were three cases of bone marrow uptake; two were attributed to metastatic disease and one, to recent treatment of leukemia. Flow chart of SUVmax range of different skeletal lesions is demonstrated in Fig 1 (b)

^{18}F FECH PET/CT data was further analysed based on avidity on PET component, detection of osteoblastic lesions on Bone Scan with a view to segregate lesions which are avid on one modality and non avid on the other and vice versa. A true matched analysis was possible in 59 /72 lesions as cases where Tc99m MDP Bone Scan was not available were excluded from the analysis. A total of 56/59 lesions were found to be avid on 18F Choline PET/CT. The SUVmax value 0.6-11.6. 37.5% (21/56 lesions) demonstrated osteoblastic activity while 62.5% (35/56 lesions) were non avid on bone scan (Fig 1c). The PSA value ranged from 0.04-372. Detailed analysis of the lesions as isodense, sclerotic, lytic, or mixed, SUVmax range, bone scan avidity and PSA values are listed in Table 1.

There were only 3 lesions which were non avid on ^{18}F FECH PET/CT but were avid on Tc99m MDP Bone Scan. All of these three were sclerotic lesions, SUVmax range was 1.06-1.08 and PSA value was 3.6-240 (Table 2).

Fig. 2 shows the scatter plot of SUV_{max} values in relation to lesion characterization as benign or malignant. We noted minimal overlap of benign and malignant lesions was seen above SUVmax of 2.5.

DISCUSSION

To our knowledge this is the first study to analyze the correlation between lesion-based analysis of skeletal findings on low-dose CT, bone scan, and quantification data obtained with ^{18}F-FECH PET/CT. It was observed that 29% of the ^{18}F-FECH PET/CT-positive lesions had a benign etiology. The study also demonstrates the superiority of ^{18}F-FECH PET/CT over bone scan, given that bone scan detected only 37.5% of the ^{18}F-FECH-avid lesions.

The skeleton is the second most frequent site (after lymph nodes) for metastases from prostate cancer, and the incidence of skeletal involvement is 65–75% among patients with advanced disease [9] . Among the 15% of patients with bone lesions in this study, 71% of the lesions were due to metastatic disease. The distribution of skeletal lesions overlapped with the sites of spread of prostate cancer, and 43% of the lesions were seen in the pelvis (31/72 lesions) and 23.6% in the spine (17/72 lesions), with scattered foci of uptake in the remainder of the skeleton. The anatomical area covered in bone scan (skull vertex to feet) exceeds that covered on ^{18}F-FECH PET/CT (skull vertex to mid thigh). Bone scan did not detect any lesion in the lower limbs, which were not covered on ^{18}F-FECH PET/CT.

A total of 23/51 (45%) malignant lesions were noted to be sclerotic and out of these, 20.83% (15) were avid on ^{18}F-FECH PET/CT. Isodense but avid lesions fall into the category of "*discordant lesions*" and pose a different diagnostic dilemma. Detection of isodense but "neoplastic lesions" is a real challenge faced while reporting oncology scans. The majority of these lesions have a Hounsfield unit value very similar to that of

the adjacent bone matrix and these lesions are easily missed on diagnostic CT scans even when intravenous contrast is administered. Increased avidity of these lesions as detected by ^{18}F-FECH PET/CT helps to distinguish them from surrounding bone. Bone metastases undergo osteoblastic healing response with treatment. The isodense lesions may become sclerotic and these lesions can be easily labelled as progressive disease. In this study there were 13 isodense lesions (SUV_{max} range 1.1–7.65). Interestingly, out of these only 3 were avid on bone scan (23.1%) while the majority (76.9%) were non-avid. Even on retrospective review of this specific cohort of patients we were not able to identify these lesions on the low-dose CT component of the PET/CT. Focal ^{18}F-FECH in isodense lesions reflects bone marrow infiltration (Fig 5). Caution should be exercised when monitoring isodense lesions. Reduction in choline uptake with sclerosis can distinguish osteoblastic healing response from progressive disease [10] . Figures 3–6 show different examples from this study.

There were three osteoblastic lesions on Tc99m MDP Bone Scan, which were non-avid on 18^{F} FECH PET/CT. These included old fractures undergoing osteoblastic healing response. These were situated at site of sternal fracture (SUVmax 1.7, PSA 3.6), superior end plate fracture at T12 vertebra (SUVmax1.06, PSA 9.2) and right 10^{th} rib fracture (SUVmax 1.08, SUVmax 240). The patient with rib fracture had close serial follow up. This patient was also found to have a fracture of the 8^{th} rib on the same side which was only visible on the low dose CT component and non avid on Bone Scan and ^{18}F FECH PET/CT. Due to symmetrical nature but very high PSA a differential of fractures and metastatic disease was made. These were found to be stable on 3 serial Bone Scans over a

period of 2 years and also on 2 serial CT Scans over 12 months. The patient was put on hormones with gradual decline of PSA from 240 to 29.79, 13.07 and 9.14.

Our cohort demonstrated that quantification of ^{18}F-FECH uptake cannot characterise skeletal lesions as benign or malignant in patients undergoing investigation for biochemical relapse of prostate cancer and furthermore does not correlate with the isodense, sclerotic, lytic, or mixed lytic/sclerotic status of the lesions.

A major limitation of our study is that the bone scan images were planar images and lacked SPECT/CT, which can help with lesion characterization. At our institution, staging investigations for prostate cancer include planar images as standard of care in the vast majority of prostate cancer patients.

Histopathological correlation was not available in all cases. Our institute is a tertiary referral center to which a heterogeneous group of patients are referred for imaging from a variety of hospitals. We relied on the low-dose CT features to characterize the patients and correlated findings with available bone scans. This approach is suboptimal, but the study demonstrates that not all avid lesions on ^{18}F-FECH PET are due to a metastatic disease process.

CONCLUSION:

^{18}F-FECH PET/CT identified bone lesions in 15% of the patients with suspected prostate cancer relapse; 71% of the lesions were due to bone metastases and 29% due to benign etiology.^{18}F-FECH PET/CT demonstrates a range of benign skeletal findings and caution should be exercised in labeling choline-avid lesions as metastatic disease. Quantification

of ^{18}F-FECH PET/CT with SUV_{max} cannot be used to characterize lesions as benign or malignant. Minimal overlap of benign and malignant lesions was seen above SUVmax of 2.5. Low-dose CT acquired as part of the PET/CT may help to characterize tracer-avid lesions. Conventional ^{99m}Tc MDP bone scan detects only 37.5% of lesions detected by ^{18}F-FECH PET/CT.

REFERENCES

[1] A. Heidenreich *et al.*, "EAU Guidelines on Prostate Cancer. Part II: Treatment of Advanced, Relapsing, and Castration-Resistant Prostate Cancer," *Eur. Urol.*, vol. 65, no. 2, pp. 467–479, Feb. 2014.

[2] L. K. Griffeth, "Use of PET/CT scanning in cancer patients: technical and practical considerations," *Proc. Bayl. Univ. Med. Cent.*, vol. 18, no. 4, pp. 321–330, Oct. 2005.

[3] H. Jadvar, "Prostate Cancer: PET with 18F-FDG, 18F- or 11C-Acetate, and 18F- or 11C-Choline," *J. Nucl. Med.*, vol. 52, no. 1, pp. 81–89, Jan. 2011.

[4] S. Fanti *et al.*, "PET/CT with (11)C-choline for evaluation of prostate cancer patients with biochemical recurrence: meta-analysis and critical review of available data," *Eur. J. Nucl. Med. Mol. Imaging*, Oct. 2015.

[5] G. Shen, H. Deng, S. Hu, and Z. Jia, "Comparison of choline-PET/CT, MRI, SPECT, and bone scintigraphy in the diagnosis of bone metastases in patients with prostate cancer: a meta-analysis," *Skeletal Radiol.*, vol. 43, no. 11, pp. 1503–1513, Nov. 2014.

[6] D. T. Price, R. E. Coleman, R. P. Liao, C. N. Robertson, T. J. Polascik, and T. R. DeGrado, "Comparison of [18 F]fluorocholine and [18 F]fluorodeoxyglucose for positron emission tomography of androgen dependent and androgen independent prostate cancer," *J. Urol.*, vol. 168, no. 1, pp. 273–280, Jul. 2002.

[7] A. Haroon *et al.*, "Multicenter study evaluating extraprostatic uptake of 11C-choline, 18F-methylcholine, and 18F-ethylcholine in male patients: physiological distribution, statistical differences, imaging pearls, and normal variants," *Nucl. Med. Commun.*, vol. 36, no. 11, pp. 1065–1075, Nov. 2015.

[8] T. Hara, N. Kosaka, and H. Kishi, "Development of (18)F-fluoroethylcholine for cancer imaging with PET: synthesis, biochemistry, and prostate cancer imaging," *J. Nucl. Med. Off. Publ. Soc. Nucl. Med.*, vol. 43, no. 2, pp. 187–199, Feb. 2002.

[9] S. Halabi *et al.*, "Meta-Analysis Evaluating the Impact of Site of Metastasis on Overall Survival in Men With Castration-Resistant Prostate Cancer," *J. Clin. Oncol. Off. J. Am. Soc. Clin. Oncol.*, vol. 34, no. 14, pp. 1652–1659, May 2016.

[10] M. Beheshti *et al.*, "The use of F-18 choline PET in the assessment of bone metastases in prostate cancer: correlation with morphological changes on CT," *Mol. Imaging Biol. MIB Off. Publ. Acad. Mol. Imaging*, vol. 11, no. 6, pp. 446–454, Dec. 2009.

Table 1

Low dose CT features of 18F FECH avid lesions	SUVmax range	Bone Scan positive	Bone Scan negative	PSA Range
Isodense 13	1.1-7.65	3 (23.07%)	10 (76.92%)	3.02-153
Sclerotic 35	0.6-11.6	14 (40%)	21 (60%)	2.81-372
Lytic 4	0.7-8.58	2 (50%)	2 (50%)	1.2-5.89
Mixed sclerotic/lytic 4	1.27-3.53	2 (50%)	2 (50%)	0.04-7
TOTAL 56	0.6-11.6	21 (37.5%)	35 (62.5%)	0.04-372

Table 2

Low dose CT Features of non avid 18F FECH Lesions showing osteoblastic activity on Bone Scan	**SUVmax range**	**PSA**
Isodense 0	NA	NA
Sclerotic 3	1.06-1.08	3.6-240
Lytic 0	NA	NA
Mixed sclerotic/lytic 0	NA	NA
TOTAL 3	1.06-1.08	3.6-240

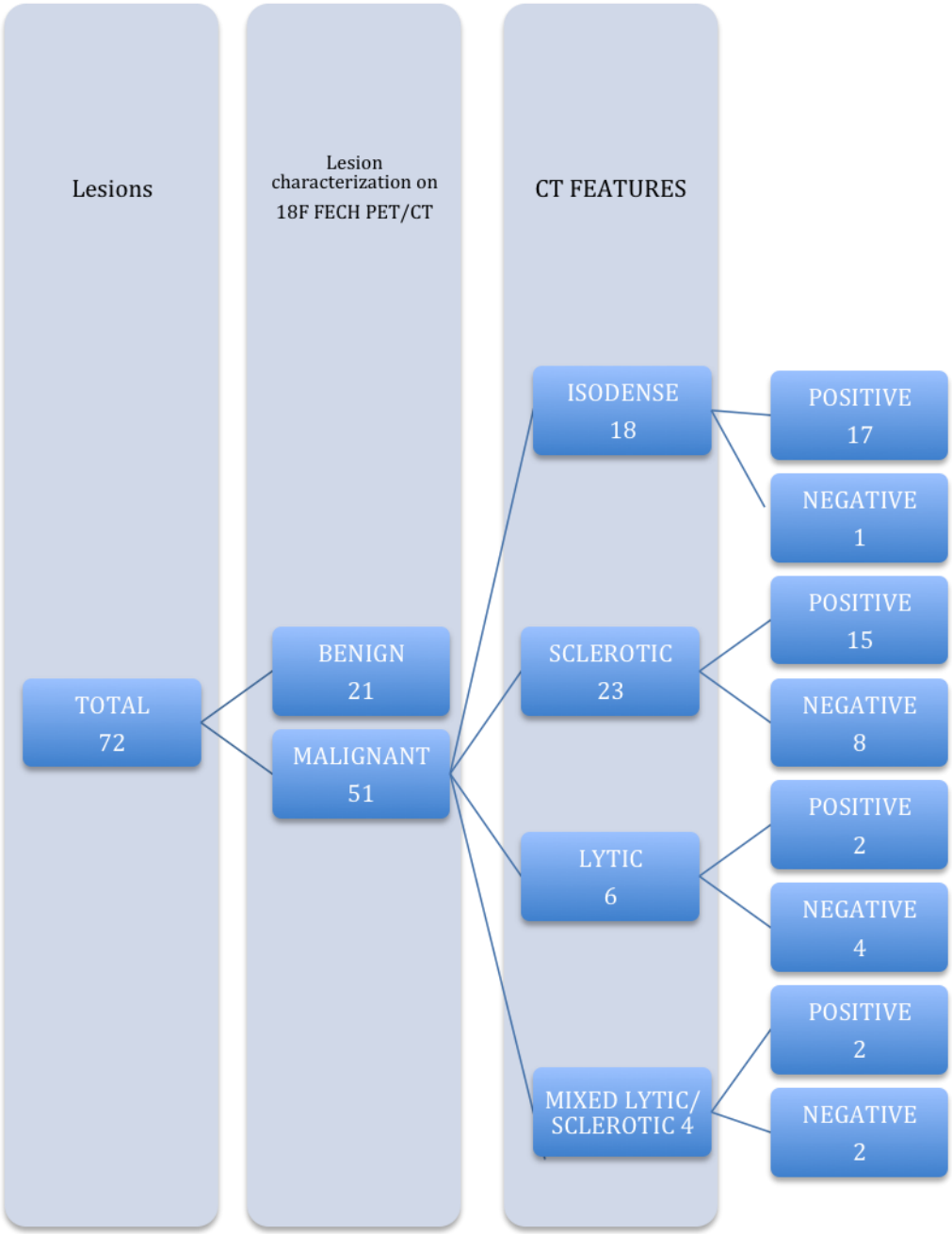

Figure 1 (a) Flow chart demonstrating distribution of the case mix in this analysis.

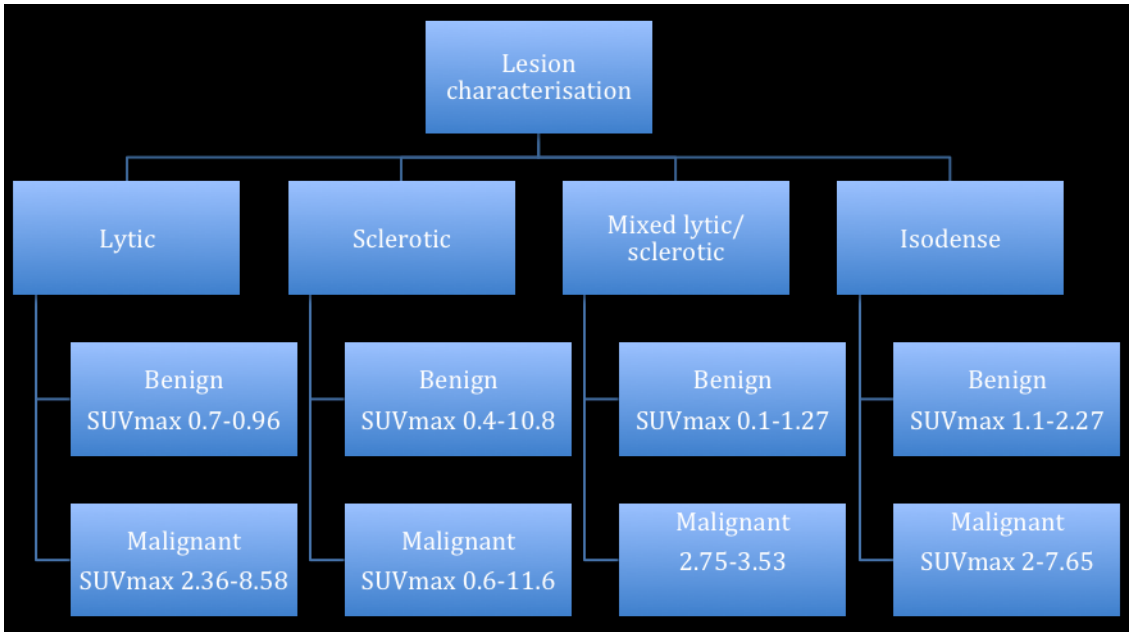

Fig 1(b) :

Flow chart of the SUVmax range of different skeletal lesions characterized as benign or malignant on the ^{18}F FECH PET/CT.

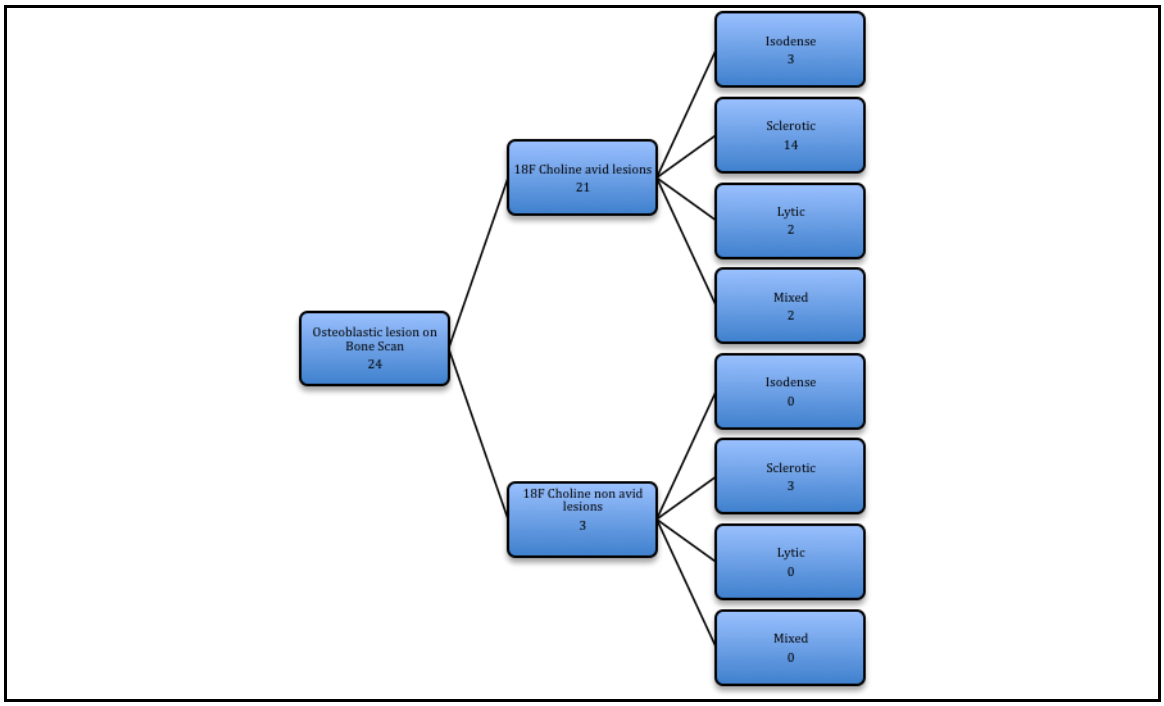

Fig 1(c):

Osteoblastic lesions and 18F Choline PET/CT. Only 3 lesions demonstrating osteoblastic activity were found to be non-avid on 18F Choline PET/CT. All three related to non - acute fractures (sternum, vertebra, rib).

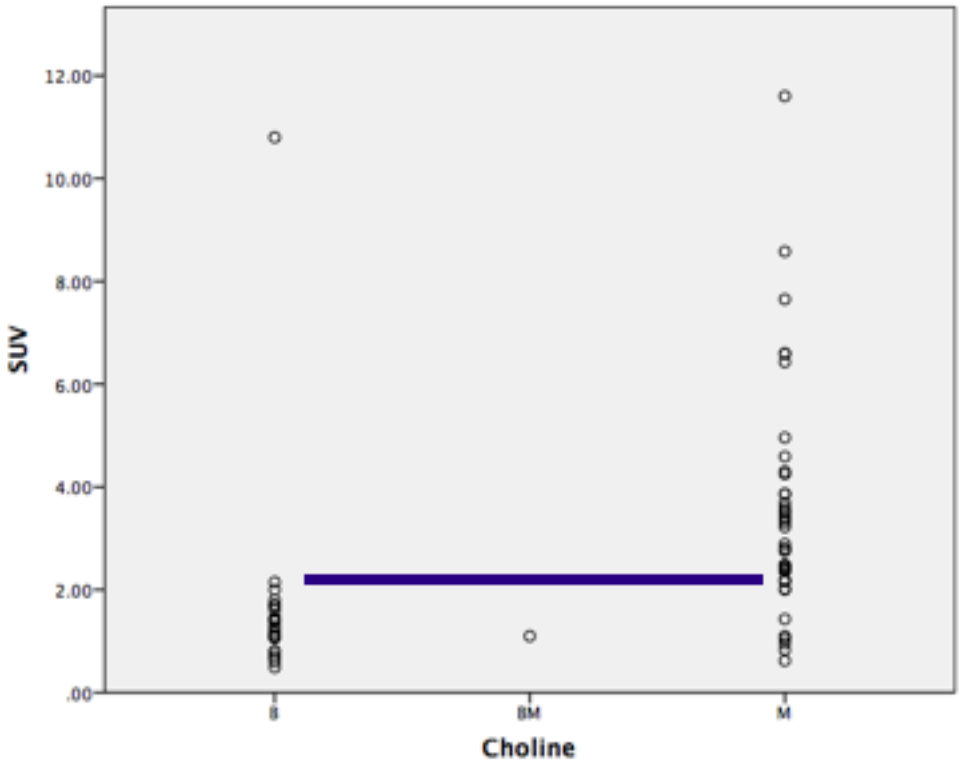

Figure 2-SUV_{max} values of benign lesions (*B*) and malignant lesions (*M*). There is an overlap of SUV_{max} values between benign and malignant lesions. The only outlier in the benign category with intense uptake was a case of fibrous dysplasia with SUV_{max} greater than 11. *BM*, bone marrow uptake.

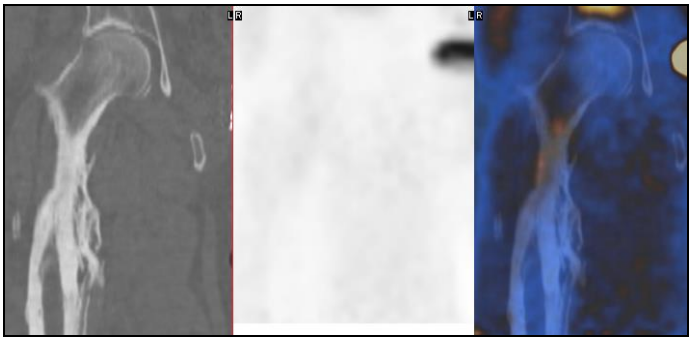

a

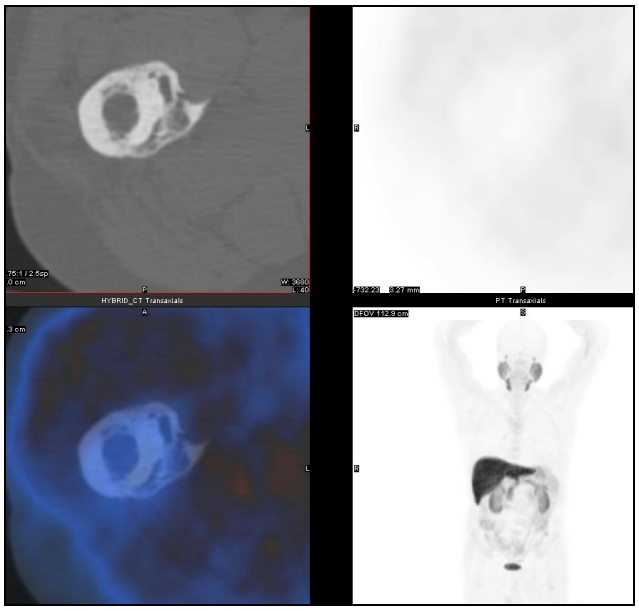

b

Figure 3a, b- Multiplanar ^{18}F-FECH PET/CT with coronal, axial, and MIP (maximum intensity projection) images showing sclerosis, periosteal thickening, and low-grade uptake at the proximal aspect of the right femur. This patient had a previous history of osteomyelitis.

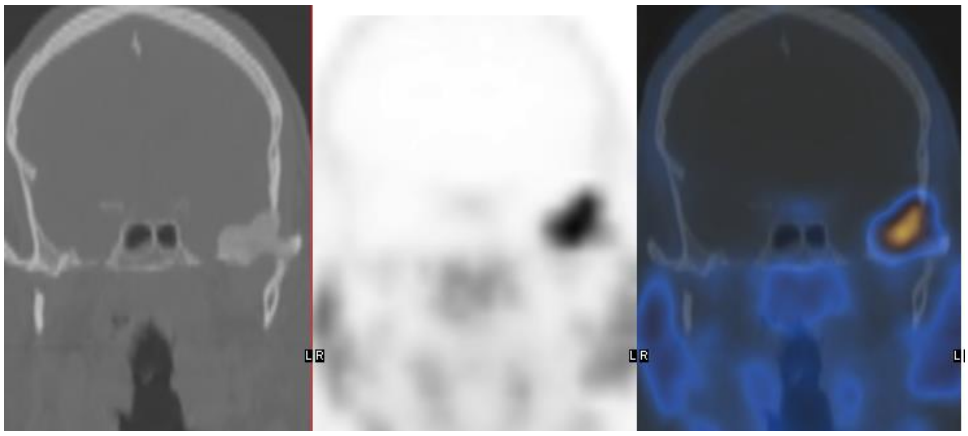

a

b

Figure 4. **a** - Coronal (low-dose CT, PET, and PET/CT) and **b** axial (low-dose CT and PET/CT) ^{18}F-FECH images showing an intensely avid area at the left skull base with ground glass appearances on low-dose CT. These findings are in keeping with fibrous dysplasia.

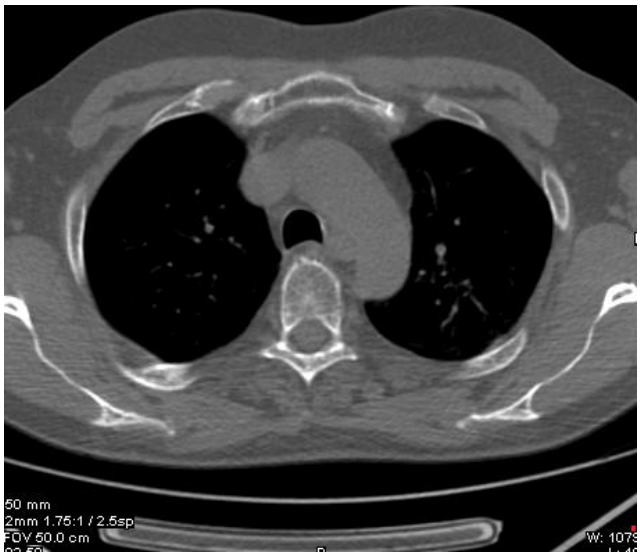

a

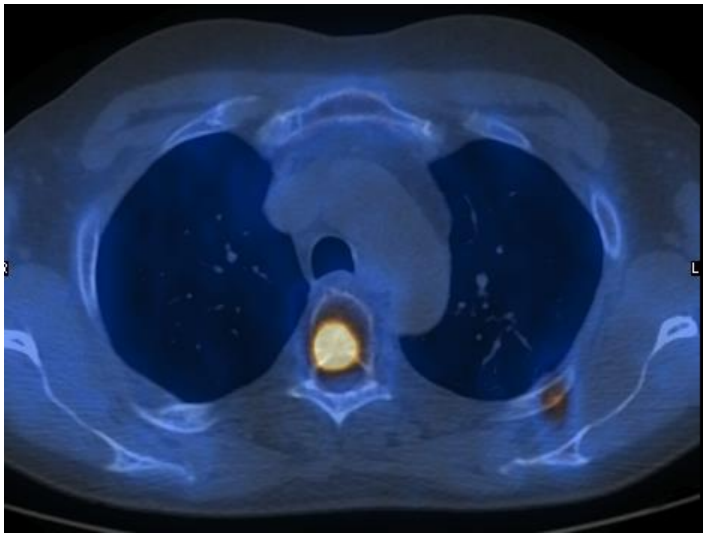
b

Figure 5: a, b On CT, there is no evidence of sclerotis, lysis, pedicular destruction, or pre- or paravertebral soft tissue abnormailty to indicate metastatic disease. **b** Axial PET/CT and low-dose CT demonstrate an intensely avid lesion at the upper thoracic vertebra, which is in keeping with metastatic disease. In addition, there is an isodense metastatic deposit involving the left 4th rib.

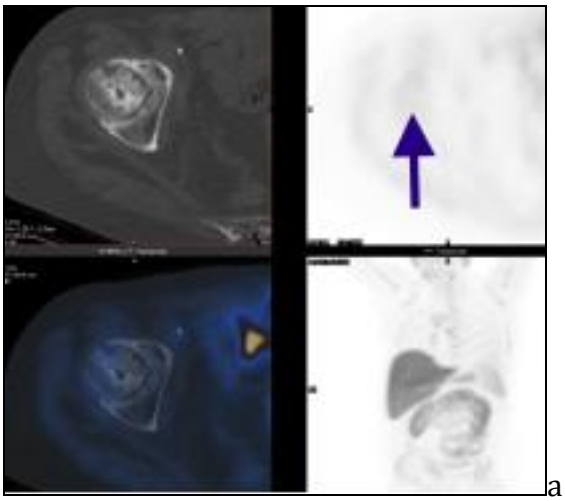
a

b

Figure 6. a -^{18}F-FECH PET/CT (multiplanar) demonstrating a very faintly avid area at the right femoral head with cystic appearances. **b** The coronal MRI scan demonstrates a focal area of low signal involving the right femoral head with loss of height. This patient had a previous history of avascular necrosis of the right femoral head.